Acta Technica *63* No. 1B/2018, 1–12

Depth computation for the onset of organic sedimentation formation in the oil producing well as exemplified by the Sibirskoye oil field

G. Korobov[1,2], D. Podoprigora[1]

Abstract. The article deals with the issues of determining fluid temperature in the flowing wells complicated by the formation of asphaltene-resin-paraffin deposits. For production conditions of the Sibirskoye Oil Field, values of heat transfer coefficient in the heat equation have been estimated by analyzing the actual temperature logs of the well. It is shown that the calculated temperature logs constructed using these values of the heat transfer coefficient are practically identical to the actual ones. The authors determined the influence of asphaltene and resin content on wax appearance temperature in the well and on the deposit formation intensity. The article demonstrates nomograms enabling to evaluate wax appearance temperature in the well based on the values of asphaltenes and resin content in oil. Impact of water cut on the deposit formation intensity in the well has been shown. Using the obtained dependencies a mathematical model was created to evaluate the depth of the onset of asphaltene-resin-paraffin deposit formation in the well with practical accuracy.

Key words. Organic deposits, asphaltenes, resins, paraffins, wax appearance temperature.

1. Introduction

The current state of development in oil fields is related to their transition to the final stage of development which is accompanied by an increase in water cut, reservoir and bottom hole pressure drop, and increase in the content of high molecular weight components in crude oil. These factors increase the risk of complications in the operation of oil producing wells due to the formation of asphaltene-resin-paraffin deposits (ARPD) on the walls of the wells and washed equipment [10]. ARPD is intensively formed when fluid temperature is lower that the wax appearance temper-

[1]Department of Development and Operation of Oil and Gas Fields, "Saint-Petersburg Mining University", Saint-Petersburg, the Russian Federation

[2]Corresponding author

ature (paraffin crystallization point) [9]. Therefore it is necessary to determine the distribution of fluid temperature and wax appearance temperature in production wells with sufficiently practical accuracy. Currently the research of temperature distribution along the hoist resulted in a significant number of solutions to heat equation describing the temperature processes occurring during the movement of products along the production wellbore. Mishchenko [8] calculate the temperature distribution along the borehole as follows:

$$\frac{t}{t_{\mathrm{bh}}} = 1 - \frac{\mathrm{wh}}{t_{\mathrm{bh}}} \cdot \frac{h}{D} \cdot \frac{K\pi D^2}{4q\rho c}\,, \tag{1}$$

where t is the fluid temperature in wellbore cross-section at a distance h from the bottomhole (°C), t_{bh} is the bottomhole temperature (°C), w denotes the geothermal coefficient of rocks surrounding the borehole (°C/m), D stands for the borehole diameter (m), q is the volume flow rate for fluids (m^3/s), ρ denotes the fluid density (kg/m^3), c stands for the fluid heat capacity (J/K), and K denotes the heat transfer coefficient (W/(m^2 °C). The heat transfer coefficient K remains unknown in equation (1). This coefficient depends on numerous factors which in practice cannot always be known. Despite the large number of analytical studies, field engineers do not have simple and sufficiently precise recommendations for its determination. The value of temperature is now of undoubted practical interest not only at any point in the well, but even at the wellhead with the known bottomhole temperature. In [1, 2] it is proposed to calculate flow temperature at any tubing string cross-section by the equation

$$\begin{gathered} t\,(H) = t_{\mathrm{ft}} - (L_{\mathrm{ft}} - L_{\mathrm{fn}})\,\frac{0.0034 + 0.79G\cos\theta}{10^a} - \\ - (L_{\mathrm{fn}} - L)\frac{0.0034 + 0.79G\cos\theta}{10^a}\,, \\ a = \frac{Q_{\mathrm{fl}}}{20d_{\mathrm{ps}}^{2.67}}\,. \end{gathered} \tag{2}$$

Here, L_{ft}, L_{fn} and L denote the distances from the well head to the formation top, pump fishneck and the considered cross-section in the wellbore or in the tubing string, respectively (m), G is the mean geothermal coefficient (°C/m), t_{ft} stands for the temperature of rocks at the formation top elevation (°C), d_{ps} and d_{ts} represent the inside diameter of production and diameter of the tubing strings, respectively m, θ is the average hole angle (°), Q_{fl} stands for the well fluid rate (m^3/s). The construction of downhole temperature logs in the specific conditions of various development targets with the help of the above empirical equations which are given in a number of educational and reference books may lead to results that differ materially from the actual one. Figure 1 shows the calculated temperature logs obtained by the specified dependencies (9)–(11) for producing well No. 341 of the Sibirskoye Oil Field (Perm Region). The apparent discrepancy between the calculated temperature logs and the actual one indicates that the use of known empirical equations in the conditions of Sibirskoye Oil Field leads to considerable error when calculating temperature distribution in wells.

2. Methodology

2.1. Changing wax appearance temperature

To verify the influence of asphaltene content of oil on the wax appearance temperature at the laboratory of the Department of "Development and Operation of Oil and Gas Fields", Saint-Petersburg Mining Universityan experiment is carried out to determine wax appearance temperature using the FLASS analyzer (Vinci Technologies) intended to study solids onset processes in the reservoir fluid. The plant flow sheet is shown in Fig. 1. This allows for qualitative and quantitative analysis with a full description of the asphaltene and paraffin precipitation conditions (pressure, temperature, morphology, visualization, change of structure, etc.).

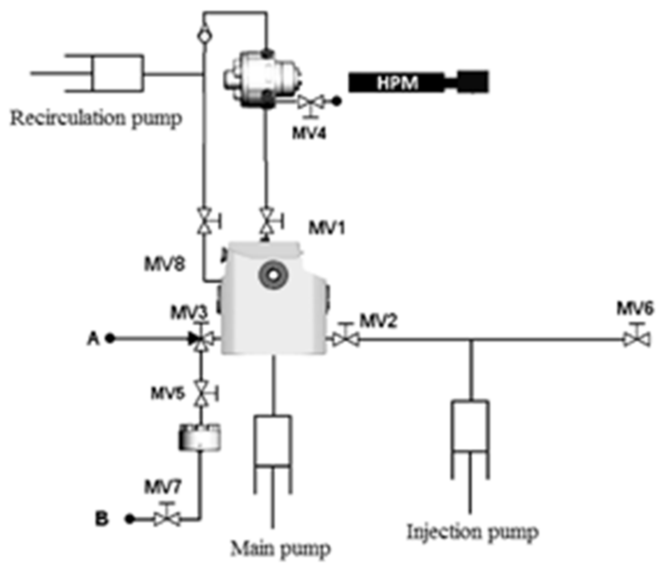

Fig. 1. FLASS system flow sheet

The measuring system includes 3 types of equipment to study solid deposition in the reservoir fluid sample:

1) High Pressure Microscope (HPM) is designed to accurately visualize paraffin and asphaltene precipitation at pressure up to 103 MPa and temperature sup to 170 °C. It enables to detect solid particles and monitor physical and morphological variations of the formed asphaltene-resin-paraffin particles with changing temperature, pressure, time and the impact of various chemical agents (CO_2, ARPD inhibitors, surfactants, solvents, etc.).

2) Solid Detection System with a laser source (SDS) is used to determine the

conditions of asphaltenes and paraffins precipitation in the reservoir fluid.

3) HPHT Organic Solid Filter is intended to determine the amount of solids formed in the fluid sample under altering PVT conditions.

Oil samples are prepared in accordance with the instructions and recommendations of Vinci Technologies Company. Sample preparation consists of heating oil samples to 90 °C in a special charging device, by means of which of oil is supplied in the PVT cell for further studies. Oil heating completely dissolve paraffins, asphaltenes and resins. After charging the PVT cell is isolated by a special high-pressure valve. Oil sample is thermostated for 24 hours in the PVT-cell. To study the paraffins and asphaltenes deposition process, SDS and HPM systems are typically used.

The general procedure for the experiments included the following:

1. To set permanent pressure in the PVT cell (an isobaric process). At the same time in case of any changes in system the pressure will be the same owing to the pump operation.

2. To reduce temperature gradually by cooling PVT cell using a temperature control system. In order to simulate the flow of oil in the well a system is included to perform continuous stirring at a certain speed. Data are recorded on the hard disk.

3. To analyze the information received for studying the conditions of asphaltene-resin-paraffin precipitation.

To determine the conditions of paraffins and asphaltenes precipitation, the isobaric method was chosen during which the system pressure is kept constant, and the temperature varies in a predetermined range. The system Pressure is selected on the basis of production data as equal to 24 MPa.

2.2. Studying intensity of asphaltene-resin-paraffin deposits formation by 'cold finger' test

To evaluate the impact of total content of asphaltenous-resinous substances (ARS) on the intensity of ARPD formation a cold finger test was conducted.

3. Results

3.1. Temperature distribution along the wellbore

While rising in the production or tubing string, fluid carries off the heat externally via the pipe wall in the elementary section of the pipe dh with lateral surface $\pi D dh$ and the amount of this heat is equal to $K\,[t_{\rm fl} - t_{\rm amb}]\,\pi D dh$. The fluid temperature decreases in this case by $c_{\rm fl}\rho_{\rm fl} v F_{\rm TR}\,{\rm d}t_{\rm fl}$. It is obvious that

$$K\,[t_{\rm lq} - (t_{\rm pl} - wh)]\,\pi D dh = c_{\rm fl}\rho_{\rm fl} v F_{\rm fl} {\rm t}_{\rm fl}\,. \tag{3}$$

Here, K is the coefficient of heat transfer from fluid to the environment, $t_{\rm fl}$ denotes the fluid temperature in the elementary section, D stands for the inside diameter of the pipe, c_{fl} is the fluid specific heat, ρ_{fl} represents the fluid density, v is the average speed of fluid flow, F_{p} denotes the pipe internal area, w is the geothermal gradient, t_{bh} represents the fluid bottomhole temperature, h is the (vertical) distance from the bottom hole to the elementary section of the pipe under consideration, t_{amb} denotes the ambient temperature (temperature of rocks at the depth $H_w - h$, H_{w} representing the well depth).

Taking into account that $vF_{\mathrm{p}} = q$ (volumetric fluid flow rate), solution of the equation (3) has the following form:

$$t_{\mathrm{fl}} = t_{\mathrm{bh}} - wh + \frac{c_{\mathrm{fl}} w \rho_{\mathrm{fl}} q}{K\pi D} - C_1 \mathrm{e}^{\frac{K\pi D h}{c_{\mathrm{fl}}\rho_{\mathrm{fl}} q}}\,, \tag{4}$$

or

$$t_{\mathrm{fl}} = t_{\mathrm{bh}} - wh + \frac{c_{\mathrm{fl}} w \rho_{\mathrm{fl}} q}{K\pi D}\big(1 - \mathrm{e}^{\frac{K\pi D h}{c_{\mathrm{fl}}\rho_{\mathrm{fl}} q}}\big)\,. \tag{5}$$

Here, C_1 is an integration constant that is determined from the initial conditions at $h = 0$, where $t_{\mathrm{fl}} = t_{\mathrm{bh}}$, therefore

$$C_1 = \frac{c_{\mathrm{fl}} w \rho_{\mathrm{fl}} q}{K\pi D}\,.$$

The heat transfer coefficient in equations (3–5) can be presented in the form of

$$K = \frac{1}{\frac{1}{\alpha} + R}\,, \tag{6}$$

where α is the coefficient of heat transfer from fluid to the internal wall of the pipe, R denotes the thermal resistance of pipe walls, annular space and borehole environment (see Fig. 2).

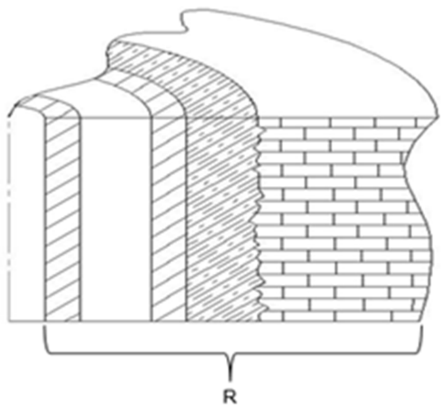

Fig. 2. Well heat transfer scheme

The coefficient α can be determined by criteria equations [5]: for a laminar flow there holds

$$\alpha = 0.021\,\mathrm{Re}^{0.8}\mathrm{Pr}^{0.43}\,\frac{\lambda_{\mathrm{f}}}{D} \tag{7}$$

and for a turbulent flow

$$\alpha = 4\frac{\lambda_{\mathrm{f}}}{D}\,. \tag{8}$$

Here, Re is the Reynolds number (similarity criterion) λ_{f} is the thermal conductivity of the pipe material and Pr is the Prandtl number (similarity criterion).

The thermal resistance R consists of resistances of tubing body, medium filling the annular space, the pipe body of the production string, cement stone and rocks surrounding the well (Fig. 2). Analytical determination of R is complicated (for the lack of information about the thermal properties of rocks surrounding the borehole, cement stone thickness is not constant; the tubing is not strictly centered in the production string, etc.).

Available actual temperature logs are used to evaluate the thermal resistance R. When solving the reverse problem using formulas (3), (4) and actual temperature log thermal, resistance R is determined.

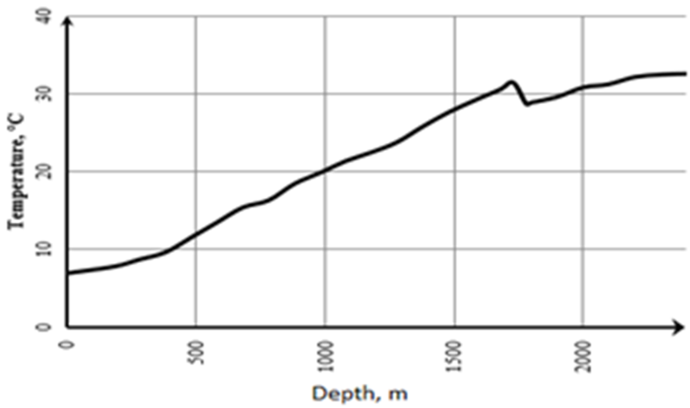

Fig. 3. An example of a downhole temperature log

The thermal resistance has no constant value along the well depth, since in different intervals it is composed of different constituents. Therefore, when determining thermal resistance, separate intervals (sections) should be singled out in the well [3]:

1 – from the bottomhole to the pump (tubing string shoe),

2 – from the pump to the dynamic head,

3 – from the dynamic head to the wellhead (see Fig. 4).

The thermal resistances of separate intervals for the studied 10 wells at Sibirskoye Oil Field are determined based on actual temperature logs by data averaging (see Fig. 4). The following values of R were obtained for the intervals [3]:

With regard to the determined thermal resistance calculation of temperature distribution is shown as exemplified by well No. 341 of the Sibirskoye Oil Field (Fig. 5). The figure shows the actual temperature log and calculated temperature logs built according to the technique proposed by Mishchenko [6] and Lyapkov for comparison [1].

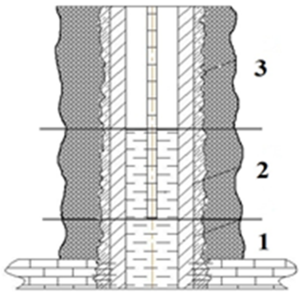

Fig. 4. Singling out well intervals during determination of resistance R: $R_1 = 0.0763\,\mathrm{m}^2\,{}^\circ\mathrm{C})/\mathrm{W}$, $R_2 = 0.0774\,\mathrm{m}^2\,{}^\circ\mathrm{C})/\mathrm{W}$, $R_3 = 0.0763\,\mathrm{m}^2\,{}^\circ\mathrm{C})/\mathrm{W}$

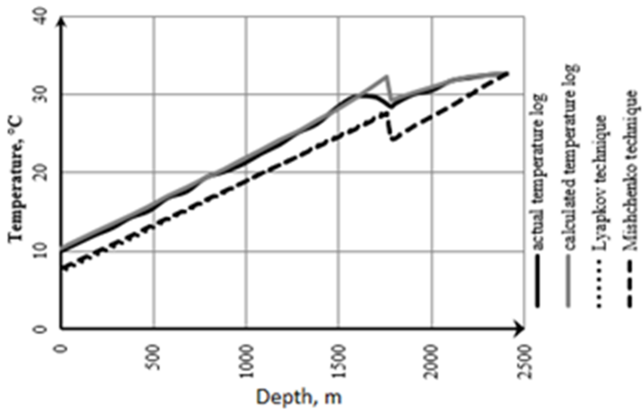

Fig. 5. Temperature logs of well No. 341, Sibirskoye Oil Field

3.2. Calculating wax appearance temperature distribution along the producing wellbore

To study the impact of asphaltenous-resinous components in oil on the process of asphalt, resin, and paraffin deposits formation, 5 more oil samples are taken. Oil samples were taken at one of the oil fields complicated with ARPD precipitation. Some data on the properties of these oil samples are given in Table 1.

Table 1. Properties and composition of oil samples

Sample number	1	2	3	4	5
Density (g/cm^3)	0.826	0.894	0.815	0.829	0.846
Dynamic viscosity (mPa s)	7.57	42.68	5.25	13.1	7.27
Contents					
paraffins (% wt)	5.9	5.6	8.1	7.8	4.5
asphaltenes (% wt)	1.6	3.6	0.6	1.8	3.3
resins (% wt)	2.8	9.5	2.5	3.5	4.5

By mixing samples specified in Table 1, two oil models were obtained (model A and model B), differing from each other in the content of asphaltenes (with similar content of resins and paraffins). Mixing samples No. 1, No. 2, and No. 3 in the proportions of 0.75, 0.18, 0.07, respectively, enabled to obtain oil model A. Mixing samples No. 1, No. 4, No. 5 in the proportions of 0.04, 0.44 and 0.52, respectively, enabled to obtain oil model B. The proportions are selected such that the resulting oil models A and B have the same content of paraffins and resins with different content of asphaltenes. The data about the content of high molecular weight components in the oil models (A, B) are given in Table 2.

Table 2. Content of high molecular weight components in the oil models (A, B)

Oil model	A	B
Proportions	1:2:3=0.75:0.18:0.07	1:4:5=0.04:0.44:0.52
Contents		
paraffins (% wt)	6	6
asphaltenes (% wt)	1.9	2.6
resins (% wt)	4	4

In further studies similar content of paraffins and resins with different content of asphaltenes in the oil model allows obtaining the dependence of any indicator on the content of asphaltenes in oil and eliminate the impact of paraffin and resin content in oil on this property. Prepared oil models (A, B) were used to assess the impact of asphaltene content on the ARPD formation process. Field data analysis shows that intensive ARPD formation occurs at fluid temperature below the wax appearance temperature [9]. To study the impact of resins content in oil on its paraffin saturation point two models are obtained. The proportions were selected so that the resulting oil models C and D have the same content of paraffins and asphaltenes with different content of resins. Data about the content of high molecular weight components in the oil models (C, D) are given in Table 3.

Table 3. Content of high molecular weight components in the oil models (C, D)

Oil model	C	D
Proportions	1:2:3=0.38:0.51:0.11	1:4:5=0.11:0.41:0.48
Contents		
paraffins (% wt)	6	6
asphaltenes (% wt)	2.5	2.5
resins (% wt)	3.5	6.2

In further studies similar content of paraffins and asphaltenes with different content of resins in the oil model allows obtaining the dependence of any indicator on the content of resins in oil and eliminate the impact of paraffins and asphaltenes in oil on this property. As a result of the experiment, the plot of paraffin wax appearance temperature versus the content of asphaltenes was built (see Fig. 6).

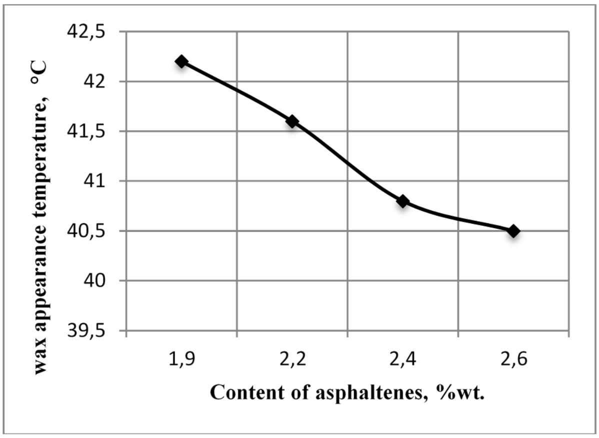

Fig. 6. Wax appearance temperature vs asphaltene content in oil

Experimental results relating to the evaluation of resin content impact on the wax appearance temperature, with isobaric decrease in temperature and at pressure of 24 MPa are shown in Fig. 7.

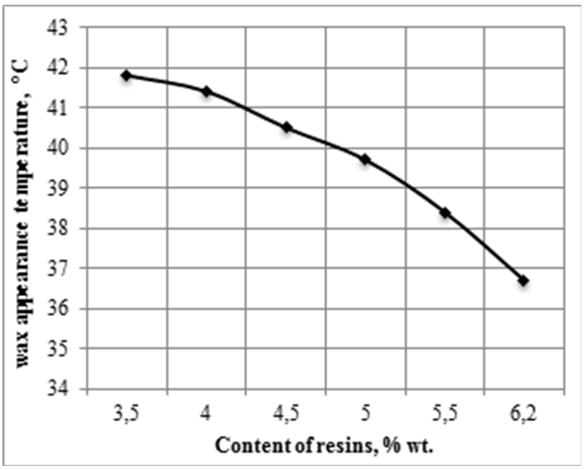

Fig. 7. Wax appearance temperature vs. resins content in oil

Most mathematical models used to determine the wax appearance temperature either do not take into account the content of asphaltenes and resins for the calculation, or relationship between the wax appearance temperature of oil and ARS content in it contradicts to the results obtained in this work. To determine wax appearance temperature with regard to the obtained relationships, a nomogram was built (see Fig. 8) that allows determining wax appearance temperature with practical accuracy. This relationship is valid for calculation of wax appearance temperature for oil with paraffin content ranging from 4.5 to 7.5 % wt and asphaltenous-resinous substances ranging from 4.5 to 13 % wt.

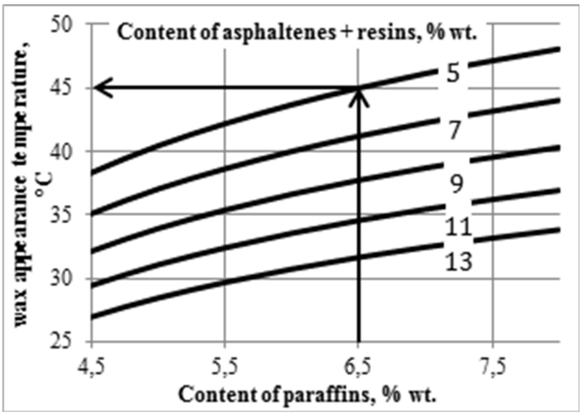

Fig. 8. Nomogram to determine wax appearance temperature

The above nomogram allows determining the wax appearance temperature in the well as a function of the content of paraffins, asphaltenes, and resins. Depth of ARPD formation is determined graphically intersection of the well temperature distribution curve and wax appearance temperature distribution curve. This method enables to consider a large amount of data while determining the ARPD formation depth:

$$H_{\text{ARPD}} = f(P_i, T_i, \Gamma_i, \Delta T_{\text{escp}}, Q_{\text{fl}}, \beta_{\text{fl}}, \eta_{\text{p}}, D_{\text{ts}})\,, \tag{9}$$

where P_i is the fluid flow pressure in the well, T_i denotes the fluid flow temperature, G_i represents the gas content in fluid flow, ΔT_{escp} stands for the thermal heating of electrical submersible centrifugal pump, Q_{fl} is the fluid rate, β_{fl} denotes the fluid water cut, η_{p} represents the pump efficiency, and D_{ts} stands for the tubing diameter.

The depth of ARPD formation on set was determined by means of model (5) for the Shershnevskoye Oil Field for 38 wells (Fig. 8). Depths of ARPD precipitation on set are plotted versus well flow rates (Fig. 9) and versus altering temperature of fluid passing through electrical centrifugal pump; it is shown that inside tubing diameter has impact on the paraffin precipitation process.

4. Conclusion

In the studied wells of the Shershnevskoye Oil Field depth of ARPD formation on set varied from 500 to 1200 m. Figure 9 shows the trend of ARPD precipitation depth decreasing with the growth of the well flow rate (approximately 8 meters per 1 m^3/day of the flow rate increase).

The described mathematical model allows for predicting the depth of the onset of the formation of ARPD in the well, and reducing the risk of complications associated with the ARPD formation, enabling to select the operating parameters of the downhole equipment in view of the possible complications during the operation of wells.

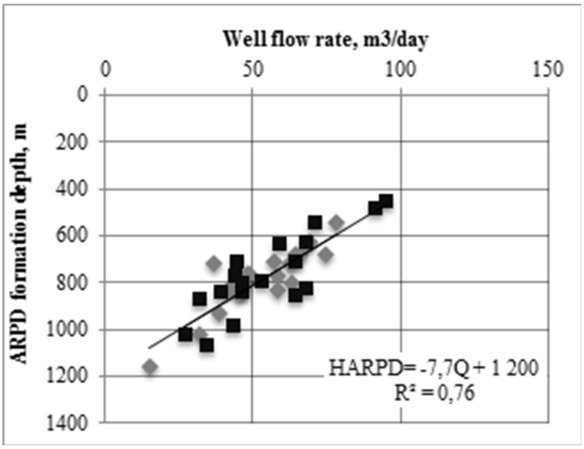

Fig. 9. Relationship between ARPD precipitation depth and well flow rates

References

[1] A. N. Zotov, K. R. Urazakov, E. B. Dumler: *Simulation of operation of pneumatic compensator with quasi-zero stiffness in the electric centrifugal submersible pump unit*. Journal of Mining Institute *229* (2018), 70–76.

[2] V. P. Tronov: *Clarification of the role of some factors influencing the process of the solid phase deposition in the flow*. Issues of Well Drilling and Oil Production: Proceedings of TatNIPIneft *5* (1964), 223–230.

[3] I. T. Mishchenko: *Downhole oil production: textbook for high schools*. Gubkin Russian State University of Oil and Gas, University Press (2007), Moscow: Oil and Gas (2007).

[4] S. K. Gimatudinov: *Reference manual of oil production*. Moscow: Knigapotrebovaniyu (2012).

[5] M. S. Kayumav: *Considerations of asphaltene-resin-paraffin deposits formation at the late stage of oil fields development*. Oil Facilities *3* (2006), 48–49.

[6] G. Y. Korobov, M. K. Rogachev: *Studying the impact of asphaltenous-resinous components in oil on the process of asphaltene-resin-paraffin deposit formation*. Petroleum Engineering *3* (2015), 162–173.

[7] G. Y. Korobov, V. A. Mordvinov: *Temperature distribution along well bore*. Oil Industry *4* (2013), 57–59.

[8] G. Y. Korobov, M. K. Rogachev: *Studying adsorption and desorption processes of asphaltene-resin-paraffin deposition inhibitor in the pore space of the carbonate reservoir*. Petroleum Engineering *1* (2016), 89–100.

[9] G. Y. Korobov, I. Raupov: *Study of adsorption and desorption of asphaltene sediments inhibitor in the bottomhole formation zone*. International Journal of Applied Engineering Research *12* (2017), No. 2, 267–272.

[10] M. A. Mikheev, I. M. Mikheeva: *Fundamentals of heat transfer*. Moscow: Energiya (1973).

Received October 12, 2017